Supporting Information for:

Perylene Diimide Aggregates on Sb-Doped SnO_2: Charge Transfer Dynamics Relevant to Solar Fuel Generation

Serena Berardi,[,†] Vito Cristino,[†] Martina Canton,[†] Rita Boaretto,[†] Roberto Argazzi,[†] Elisabetta Benazzi,[†] Lucia Ganzer,[§] Rocío Borrego Varillas,[§] Giulio Cerullo,[§] Zois Syrgiannis,[⊥] Francesco Rigodanza,[⊥] Maurizio Prato,[⊥, ^, #] Carlo Alberto Bignozzi[†] and Stefano Caramori[*,†]*

[†] Dept. of Chemical and Pharmaceutical Sciences, University of Ferrara, Via Borsari 46, 44121 Ferrara, Italy

[§] IFN-CNR, Dipartimento di Fisica, Politecnico di Milano, Piazza L. da Vinci 32, 20133 Milano, Italy

[⊥] Center of Excellence for Nanostructured Materials (CENMAT), INSTM UdR di Trieste, Dept. of Chemical and Pharmaceutical Sciences, University of Trieste, Piazzale Europa 1, 34127 Trieste, Italy

[^] Carbon Nanobiotechnology Laboratory, CIC biomaGUNE, Paseo de Miramón 182, San Sebastian, Spain

[#] Basque Fdn Sci, Ikerbasque, Bilbao 48013, Spain.

[*] Corresponding authors. E-mail: serena.berardi@unife.it; *cte@unife.it*

Index:

1. Detailed synthesis of PDI2 photosensitizer

The PDI2 photosensitizer was synthesized using a modified previously reported procedure[1-3] depicted in Scheme S1.

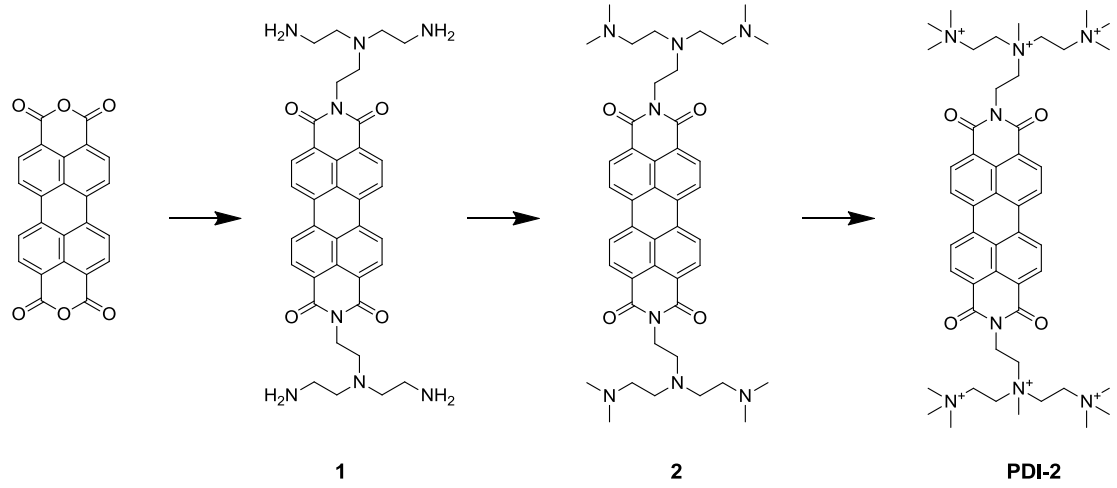

Scheme S1. Schematic synthesis of PDI2.

Perylene-*bis*-anhydride (2.0 g, 5.2 mmol), *tris*-(2-aminoethyl)amine (37 mL, 259 mmol) and imidazole (100 g) were heated at 170°C for 24 h. The reaction was cooled to RT and a mixture of ethanol and diethyl ether (1:3) was added. The mixture was filtered, washed with diethyl ether and dried under vacuum to give a red solid (**1**) in 80% yield. ^{1}H-NMR (400 MHz, CF_3COOD): δ 8.79-8.96 (m, 8H), 4.92 (m, 4H), 4.37 (m, 4H), 4.00-4.20 (m, 16H) ppm.

200 mg of **1** (0.3 mmol) were dissolved in 100 ml of a methanol/acetonitrile mixture. The solution was stirred at RT for 15 min. Formaldehyde (1.5 ml, 12 mmol) was added and stirred for one hour. 750 mg of $NaBH_3CN$ (12 mmol) were added and the solution was heated at 70°C for 16 hours. Diethyl ether was added and the precipitate was filtered and dried under vacuum to give a red solid (**2**) in 76 % yield. ^{1}H-NMR (400 MHz, CF_3COOD): δ 8.99-9.31 (m, 8H), 5.10 (m, 4H), 4.22-4.78 (m, 16H), 3.99 (m, 4H), 3.40 (s, 24H) ppm.

A mixture of **2** (150 mg, 0.2 mmol), 6 ml of MeOH and 100 mg of Na_2CO_3 was stirred at room temperature for 12 h and methyl iodide (0.5 ml) was added, heated at 60°C for 4 hours, then 72 hours at RT. The precipitated was washed with 4 x 20 mL of diethyl ether. The red solid was dried under vacuum to give **PDI2** in 61% yield. ^{1}H-NMR (400 MHz, CF_3COOD): δ 8.90-9.15 (m, 8H), 5.02 (m, 4H), 4.44 (s, 20H), 4.19 (s, 6H), 3.56 (s, 36H) ppm.

In order to exchange the anion and to make the dye soluble in acetonitrile, **PDI2** was dissolved in the minimum amount of water. In a second flask, 50 g of $(NH_4)PF_6$ were dissolved in 100 mL of water. The two solutions were mixed together and stirred for 2 hours. As soon as the two solutions were combined, a precipitate was obtained and subsequently filtered and washed with 3 x 30 mL of a $(NH_4)PF_6$ saturated solution and with 3 x 30 mL of milliQ.

2. Electrochemistry of PDI and PDI aggregates

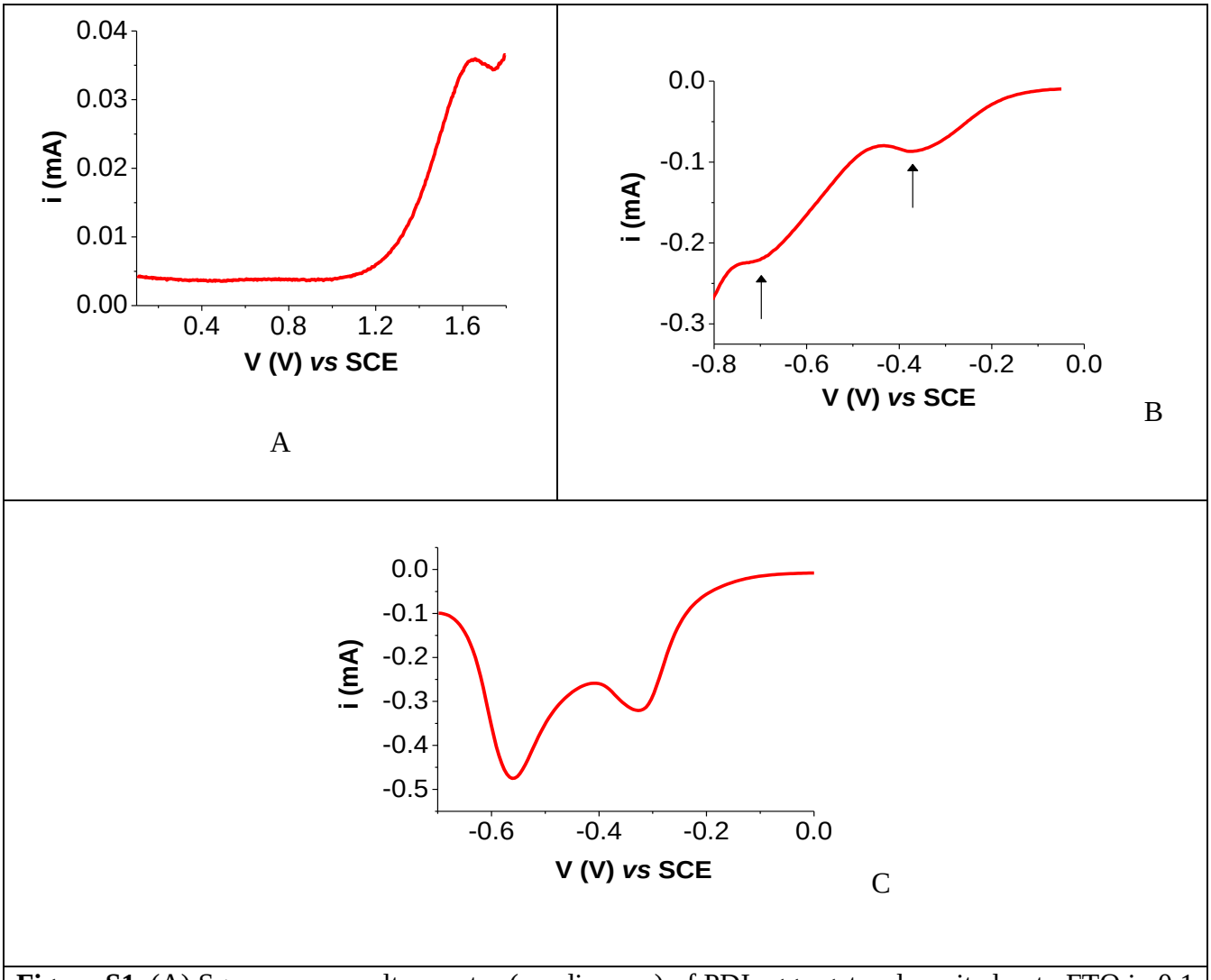

Figure S1. (A) Square wave voltammetry (anodic scan) of PDI aggregates deposited onto FTO in 0.1 M $TBAPF_6$ in ACN in order to identify the E^0_{ox}; (B-C) Square wave voltammetry (cathodic scan) of PDI aggregates deposited onto FTO, tested in either 0.1 M $TBAPF_6$ in ACN (C) or in 0.1 M NaBr (pH 1).

3. Photoanodes characterization

3.1. AFM images

ATO

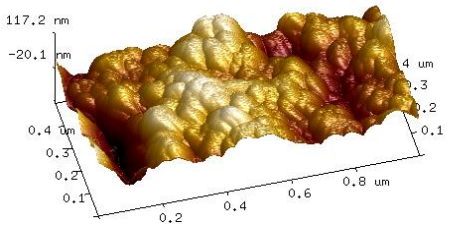

A

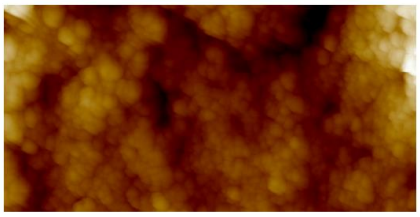

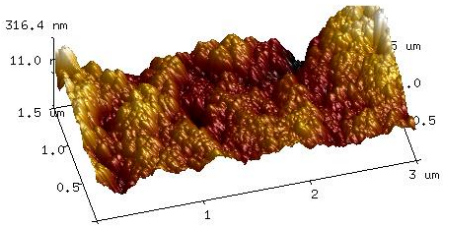

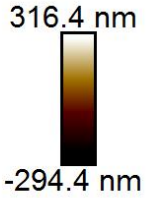

B

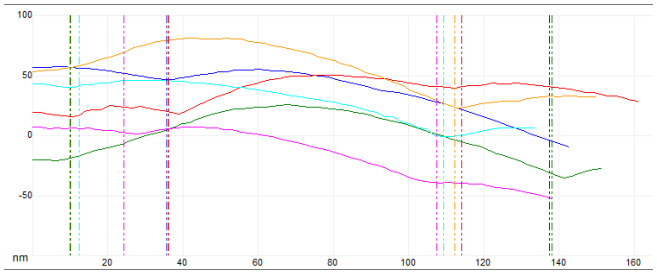

Pair	Horizontal Distance	Vertical Distance	Surface Distance
1 (blue)	101.547 (nm)	-49.865 (nm)	125.390 (nm)
2 (red)	77.733 (nm)	21.818 (nm)	95.632 (nm)
3 (green)	127.670 (nm)	-11.631 (nm)	166.847 (nm)
4 (pink)	85.258 (nm)	-42.739 (nm)	103.635 (nm)
5 (light blue)	96.080 (nm)	-42.732 (nm)	115.794 (nm)
6 (orange)	103.019 (nm)	-33.719 (nm)	137.551 (nm)

SnO_2

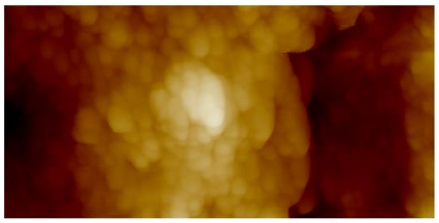

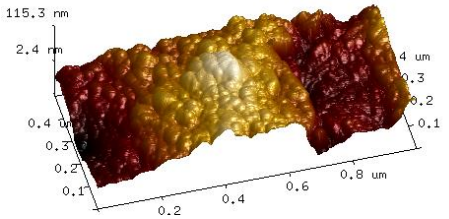

C

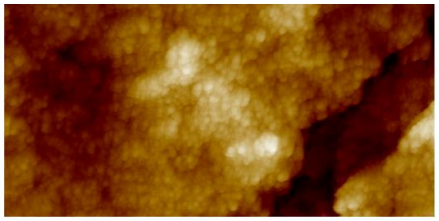

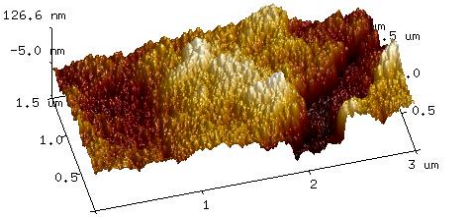

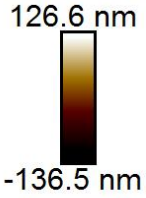

D

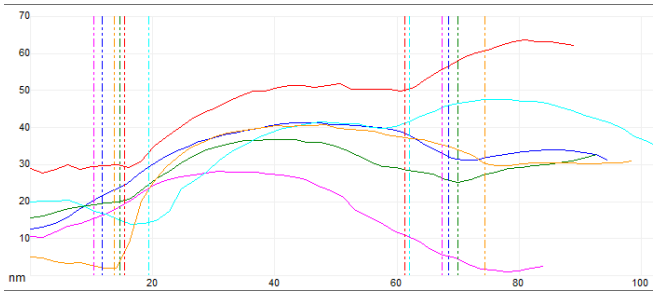

Pair	Horizontal Distance	Vertical Distance	Surface Distance
1 (blue)	57.195 (nm)	10.110 (nm)	67.037 (nm)
2 (red)	44.631 (nm)	20.558 (nm)	54.811 (nm)
3 (green)	55.707 (nm)	5.234 (nm)	65.206 (nm)
4 (pink)	57.493 (nm)	-9.847 (nm)	70.275 (nm)
5 (light blue)	43.415 (nm)	27.464 (nm)	57.074 (nm)
6 (orange)	60.450 (nm)	28.222 (nm)	87.818 (nm)

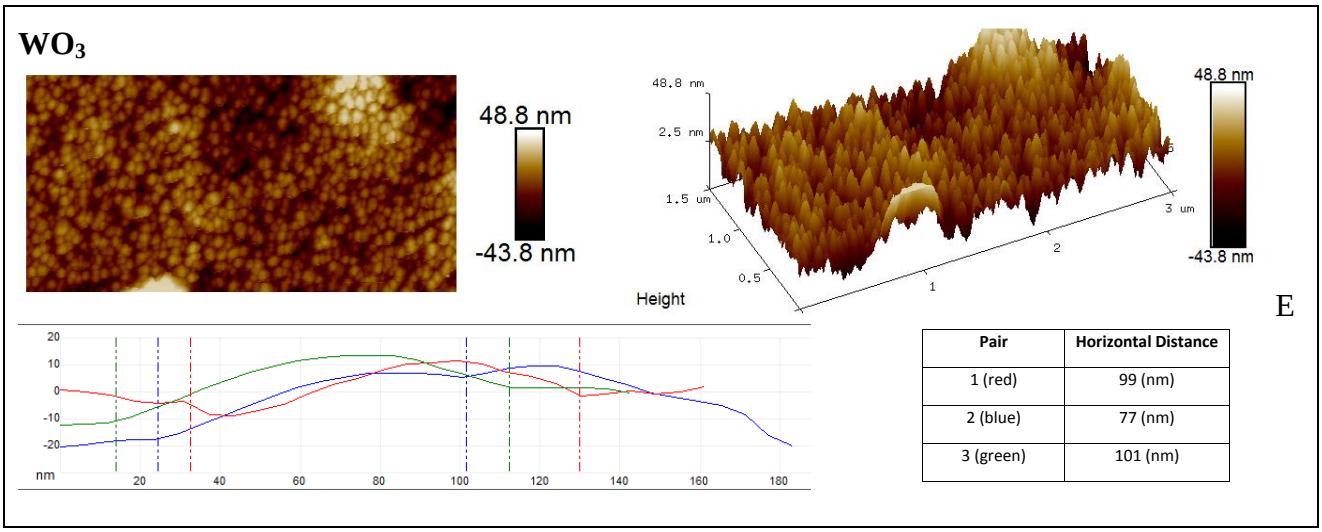

Figure S2. AFM images of the nanostructured semiconductors deposited onto FTO. A-B) ATO, 1 and 3 μm scan size respectively; C-D) SnO_2, 1 and 3 μm scan size respectively; E) WO_3, 3 μm scan size.

3.2. UV-Vis spectra of the dye-sensitized photoanodes

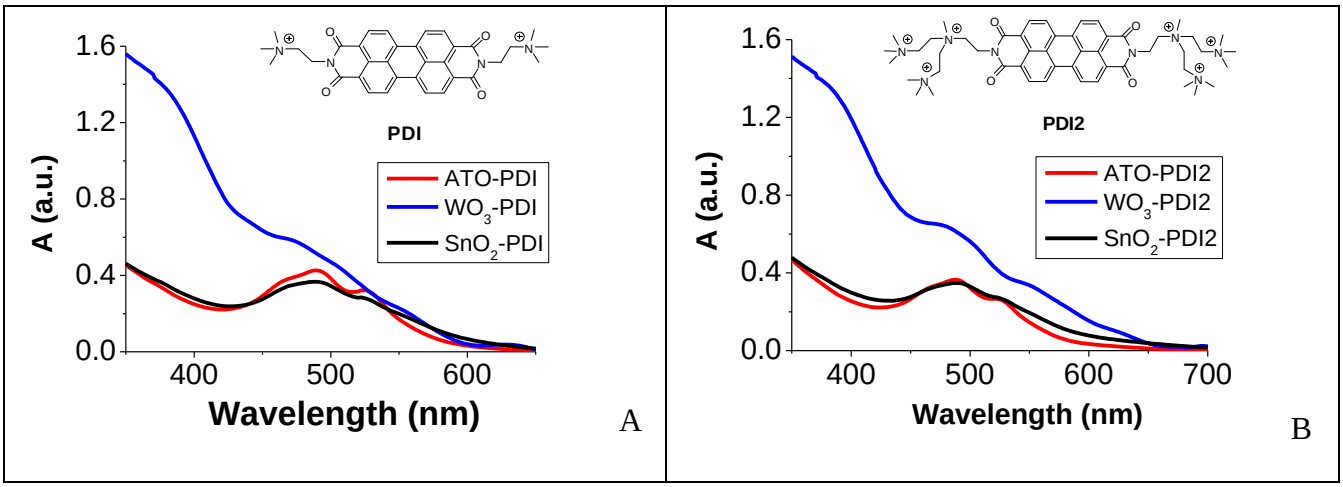

Figure S3. UV-Vis spectra of the PDI- (A) and PDI2- (B) sensitized photoanodes, not corrected for the contribution of the bare SC. Thus, in these spectra the absorptions of the dye-sensitized WO_3 photoelectrodes are the sum of the contribution of both the dye and the bare WO_3 (for $\lambda < 460$ nm).

3.3. J-V curves of the PDI-sensitized photoanodes

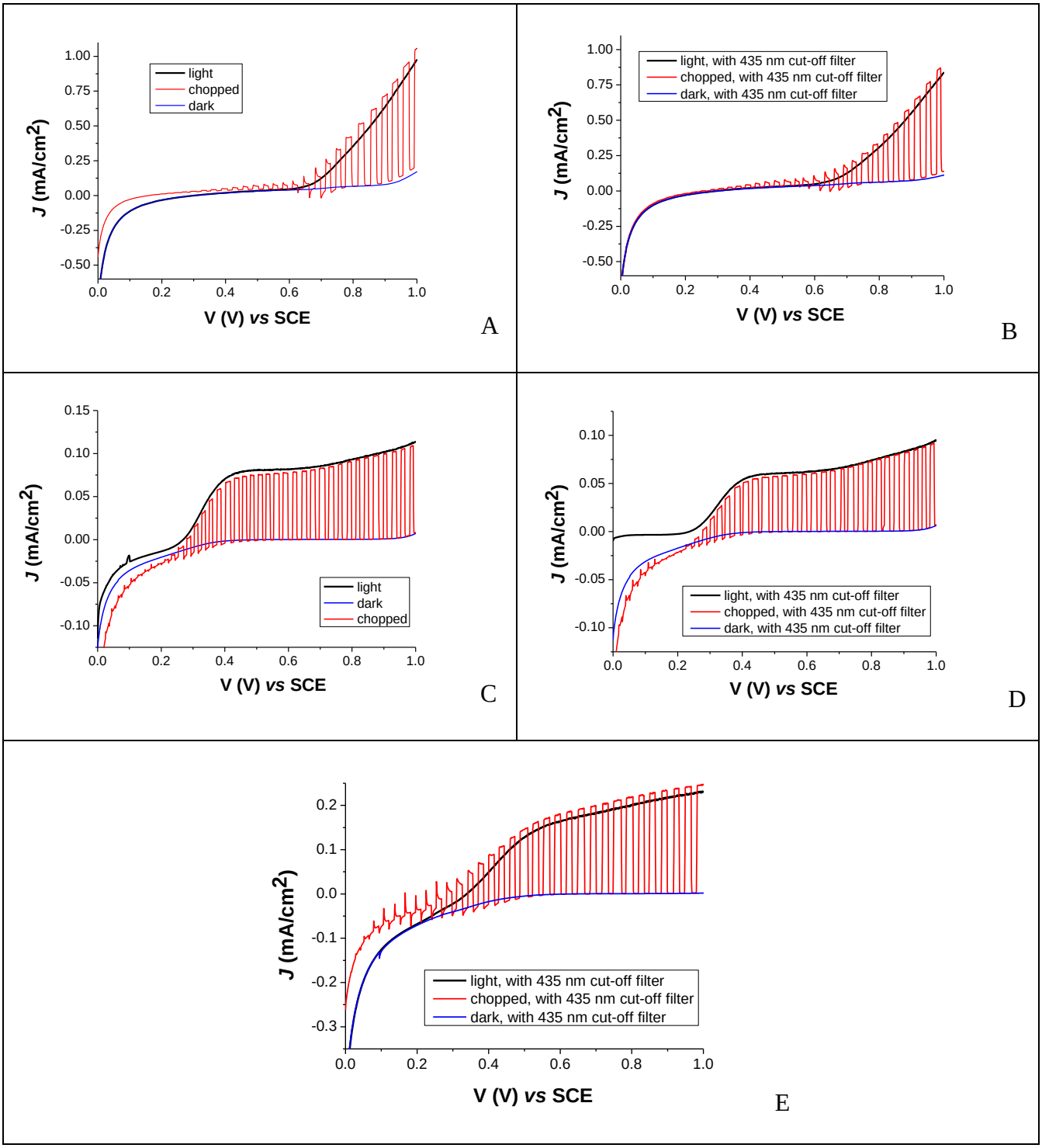

Figure S4. J-V curves of the PDI-sensitized photoanodes in 0.1 M HBr (pH 1). 10 mV/s scan rate. ATO-PDI (A) and SnO_2-PDI (C) electrodes under continuous (black) or chopped (red) illumination (0.1 W/cm^2 irradiation power, AM1.5G filter). The J-V curves registered in the presence of a further 435 nm cut-off filter are also reported for ATO-PDI (B), SnO_2-PDI (D) and WO_3-PDI (E). Dark curves in blue.

3.4. J-V curves of the PDI2-sensitized photoanodes

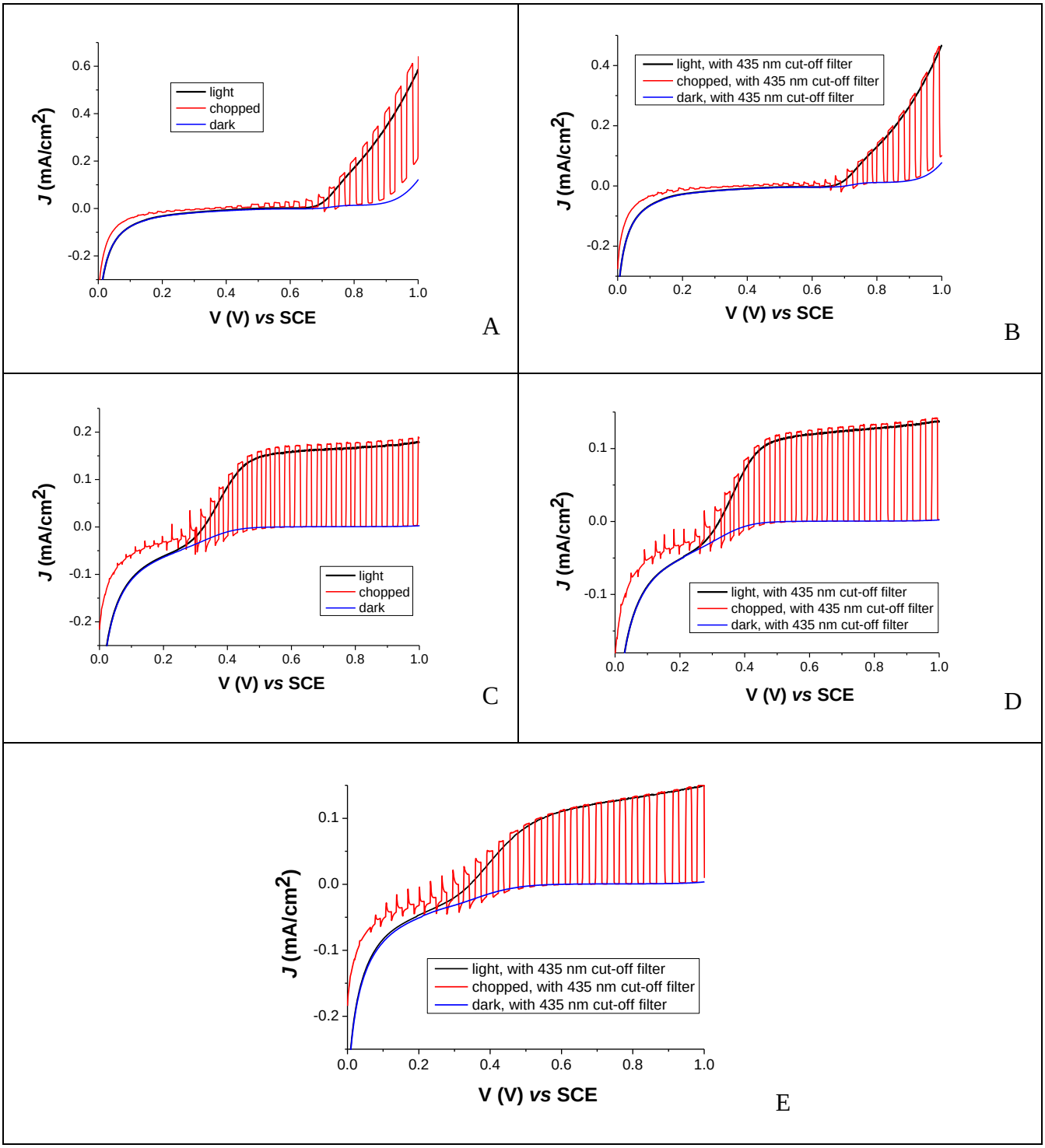

Figure S5. J-V curves of the PDI2-sensitized photoanodes in 0.1 M HBr (pH 1). 10 mV/s scan rate. ATO-PDI2 (A) and SnO_2-PDI2 (C) electrodes under continuous (black) or chopped (red) illumination (0.1 W/cm^2 irradiation power, AM1.5G filter). The J-V curves registered in the presence of a further 435 nm cut-off filter are also reported for ATO-PDI2 (B), SnO_2-PDI2 (D) and WO_3-PDI2 (E). Dark curves in blue.

3.5. IPCE/APCE curves

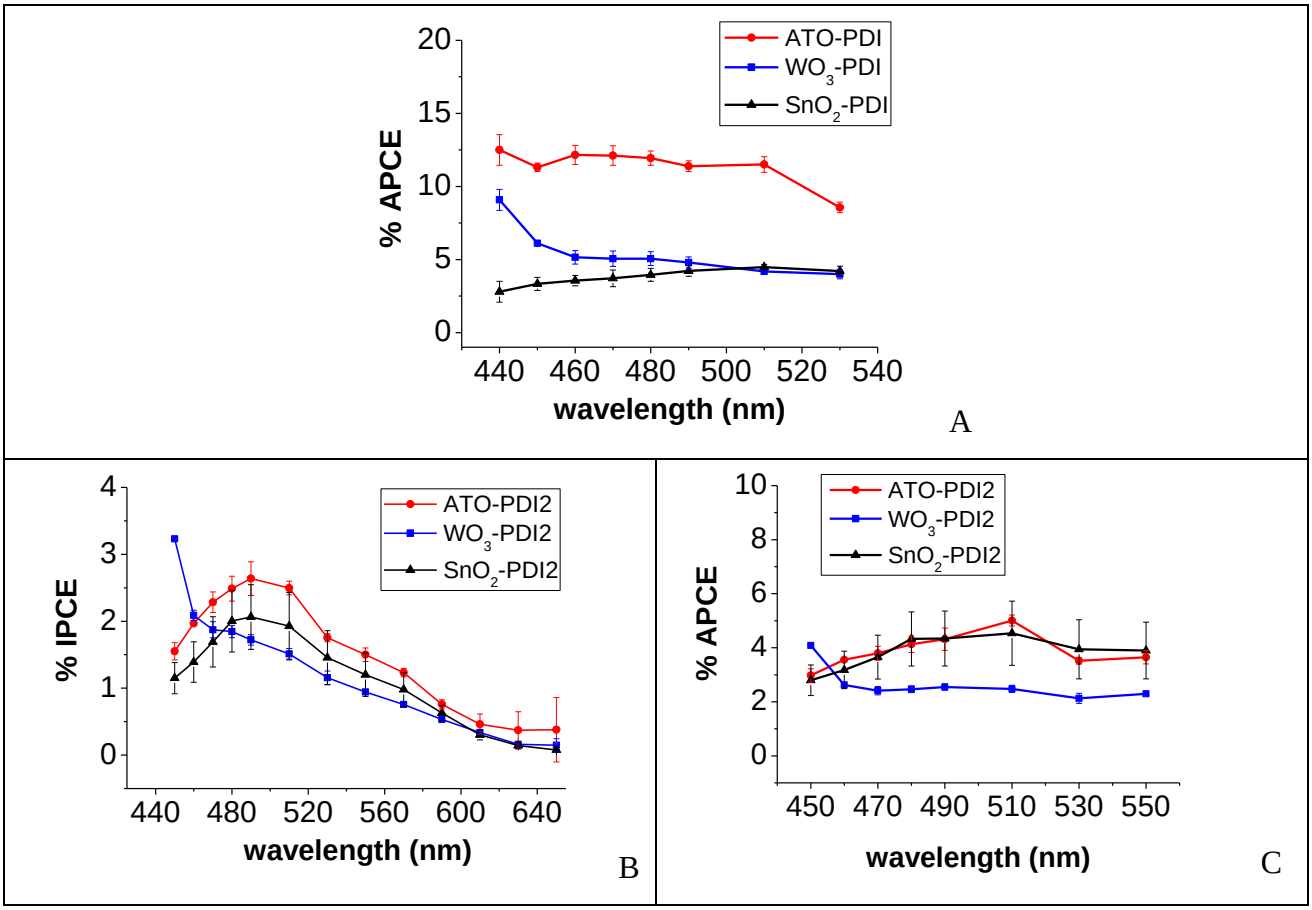

Figure S6. IPCE (A) and APCE (B-C) curves of the dye-sensitized photoanodes. Recorded in 0.1 M HBr (pH 1) under 0.8 V applied bias. Average of 2 electrodes with the corresponding error bars.

3.6. Static and time-resolved emission spectra

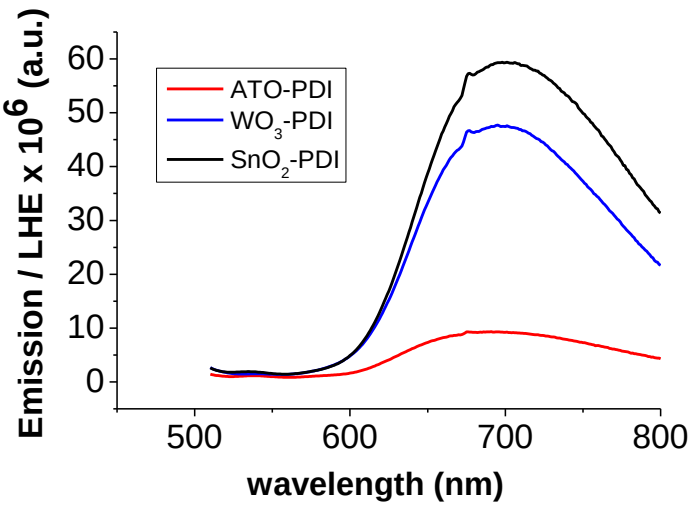

Figure S7. Emission spectra of the PDI-sensitized photoanodes. Average of two different electrodes. λ_{exc} = 485 nm.

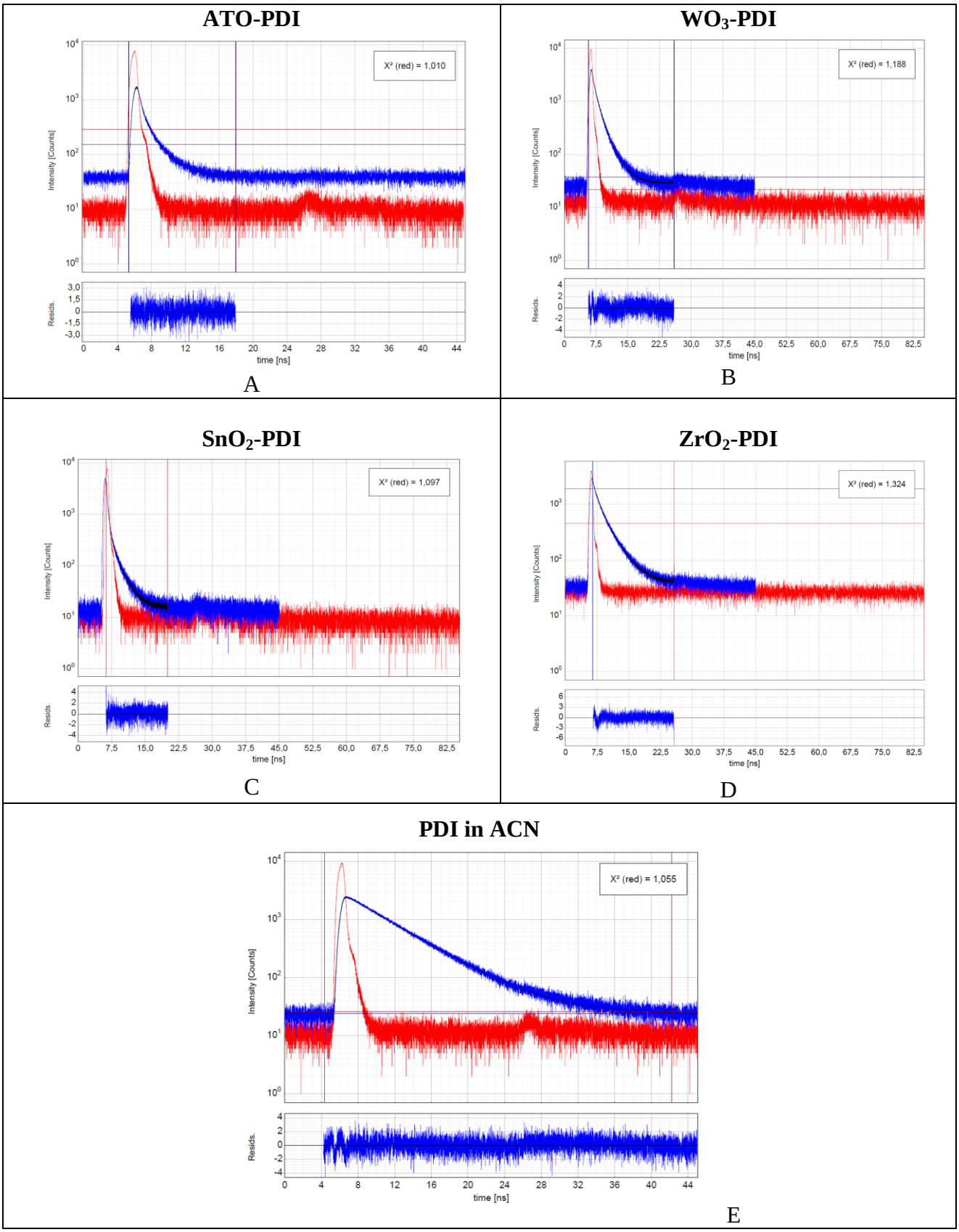

Figure S8. Fluorescence decay for ATO-PDI (A), WO_3-PDI (B), SnO_2-PDI (C) and ZrO_2-PDI (D) in 0.1 M $NaClO_4$ pH 3 (blue traces), compared to that of PDI in ACN (E, blue trace). λ_{exc} = 460 nm; λ_{probe} = 680 nm. Light source traces (red trace); exponential fittings (black trace).

3.7. Transient Photocurrent Generation

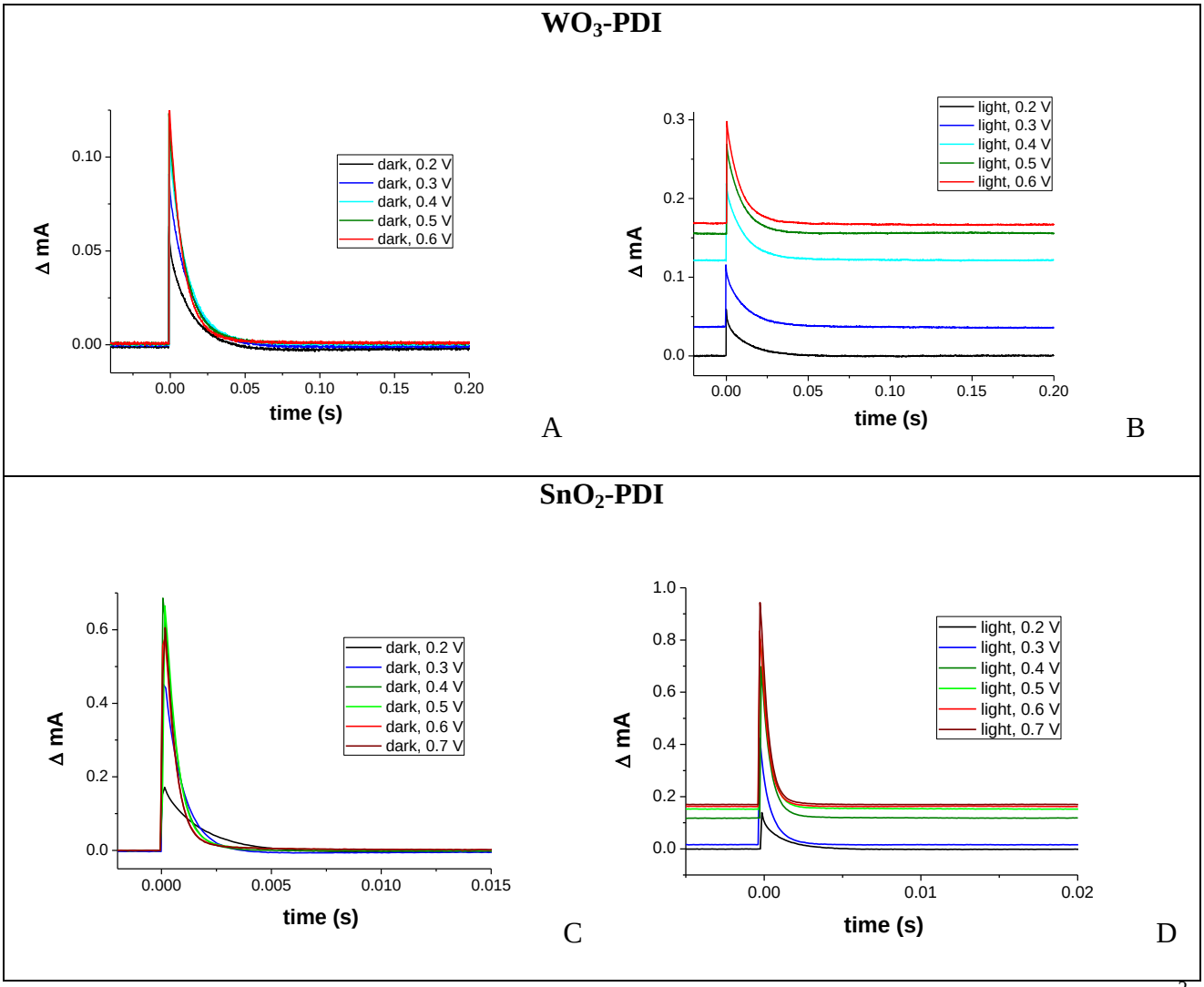

Figure S9. Photocurrent transient decays registered after the 532 nm laser excitation (0.6 mW/cm^2 intensity) under different applied bias for WO_3-PDI and SnO_2-PDI in the absence (A, C) or in the presence (B, D) of an additional white light illumination (0.14 W/cm^2 intensity). In 0.1 M HBr, pH 1.

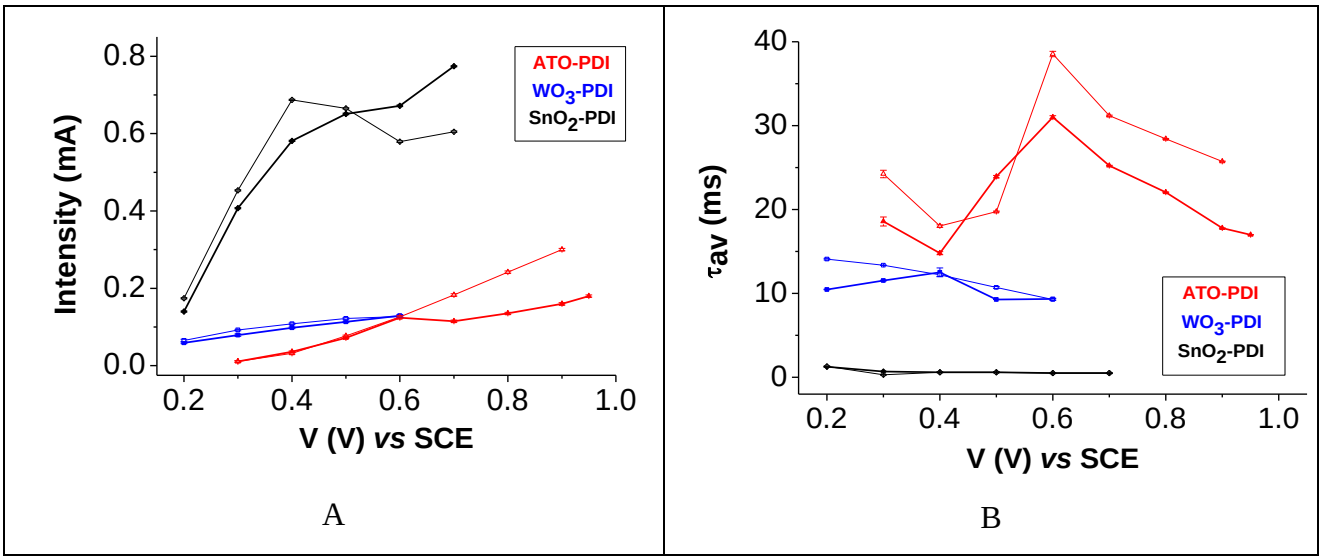

Figure S10. Rise intensity (A) and amplitude weighted lifetimes τ_{av} (B) as a function of the applied bias for the dye-sensitized photoanodes under pulsed 532 nm laser excitation (0.6 mW/cm^2 intensity) in the absence (empty markers) or in the presence (full markers) of an additional white light illumination (0.14 W/cm^2 intensity). In 0.1 M HBr, pH 1.

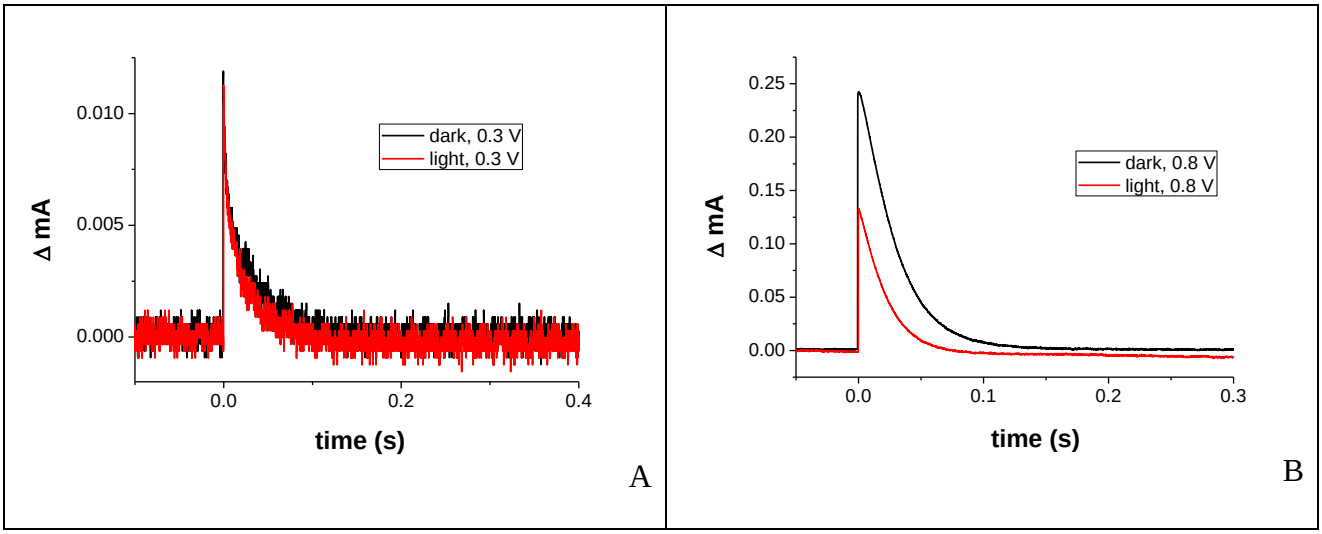

Figure S11. (A) Photocurrent transient decays of ATO-PDI after 532 nm laser excitation (0.6 mW/cm^2 intensity) under 0.3 V in the absence (black) or in the presence (red) of continuous white light illumination of 0.14 W/cm^2 intensity. In 0.1 M HBr, pH 1. (B) Traces reported in the inset Figure 2B (main text) translated to the same baseline (arbitrarily set to 0) for sake of better comparison.

3.8. Femto- and Nano-second transient absorption spectra and kinetics

ZrO_2-PDI

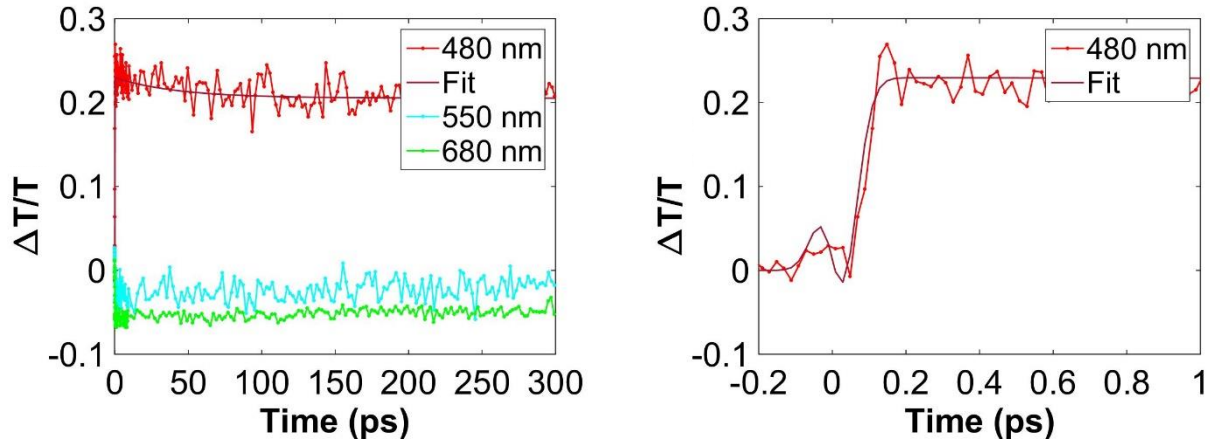

A

ATO-PDI

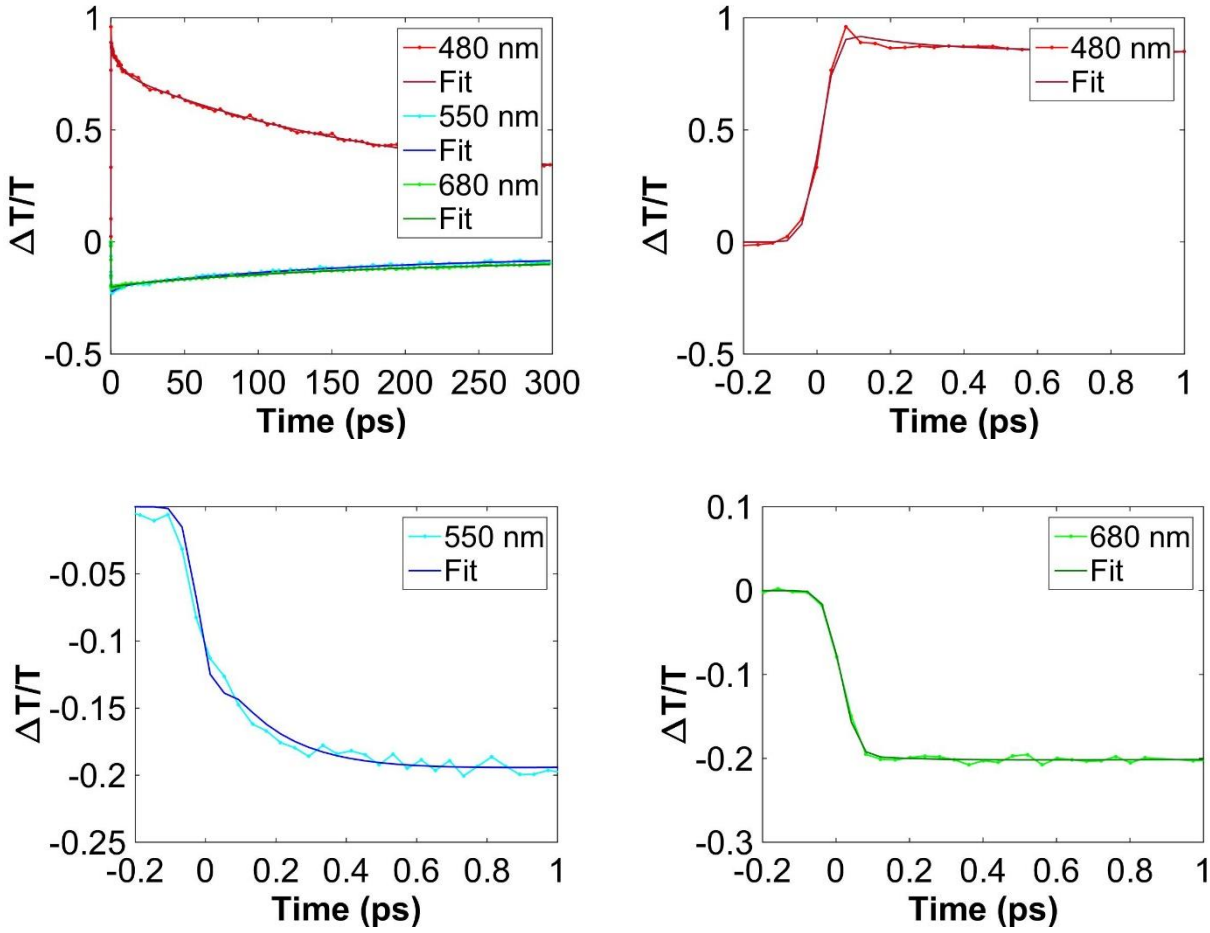

B

WO_3-PDI

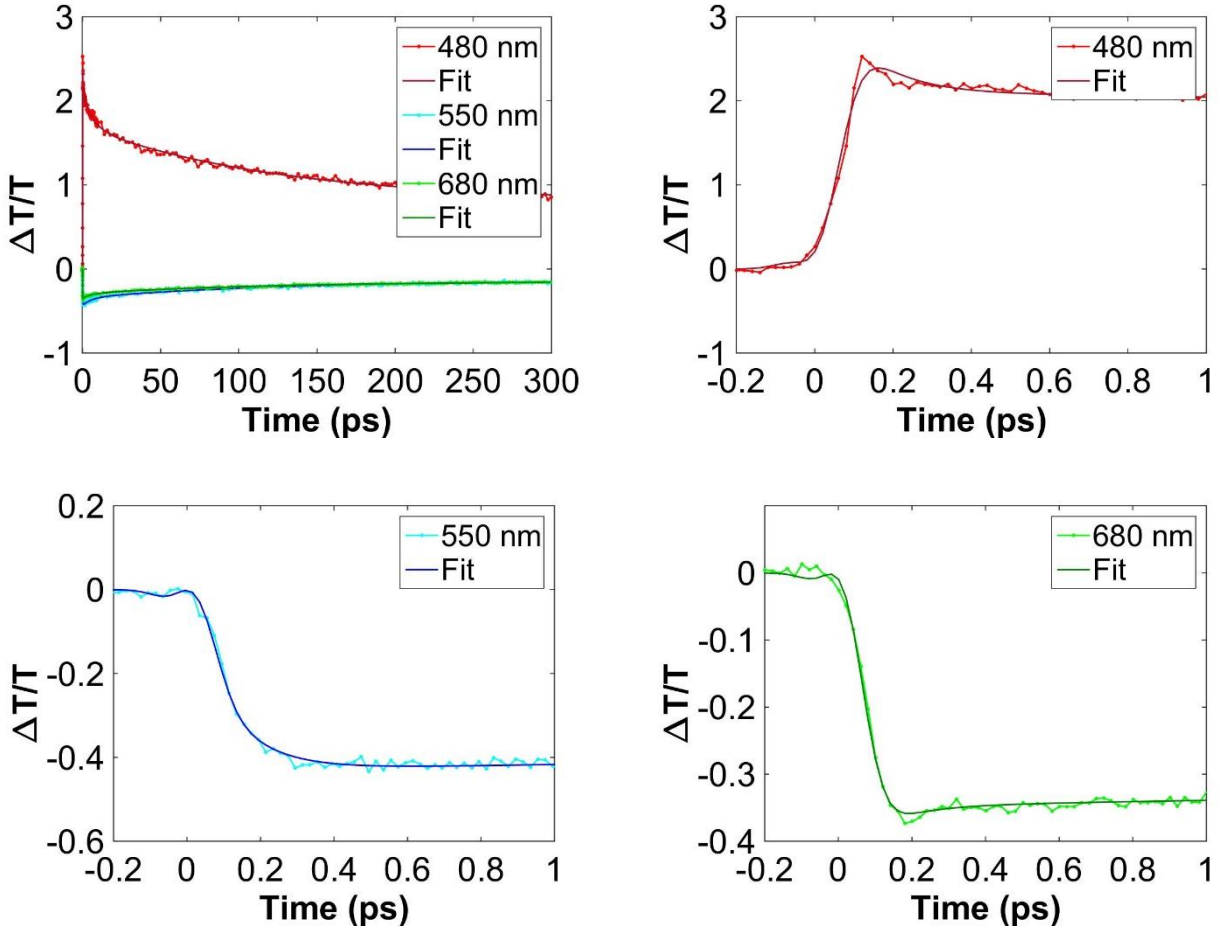

C

SnO_2-PDI

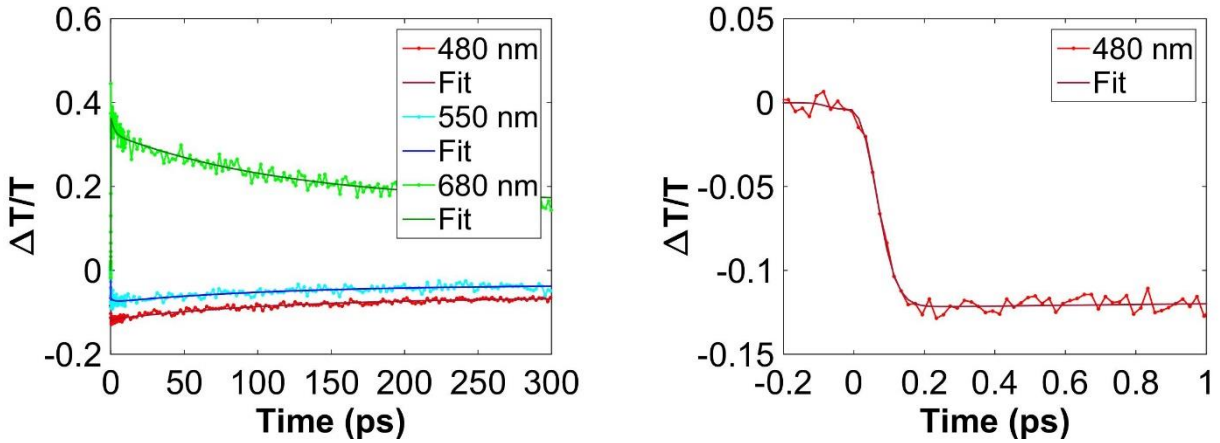

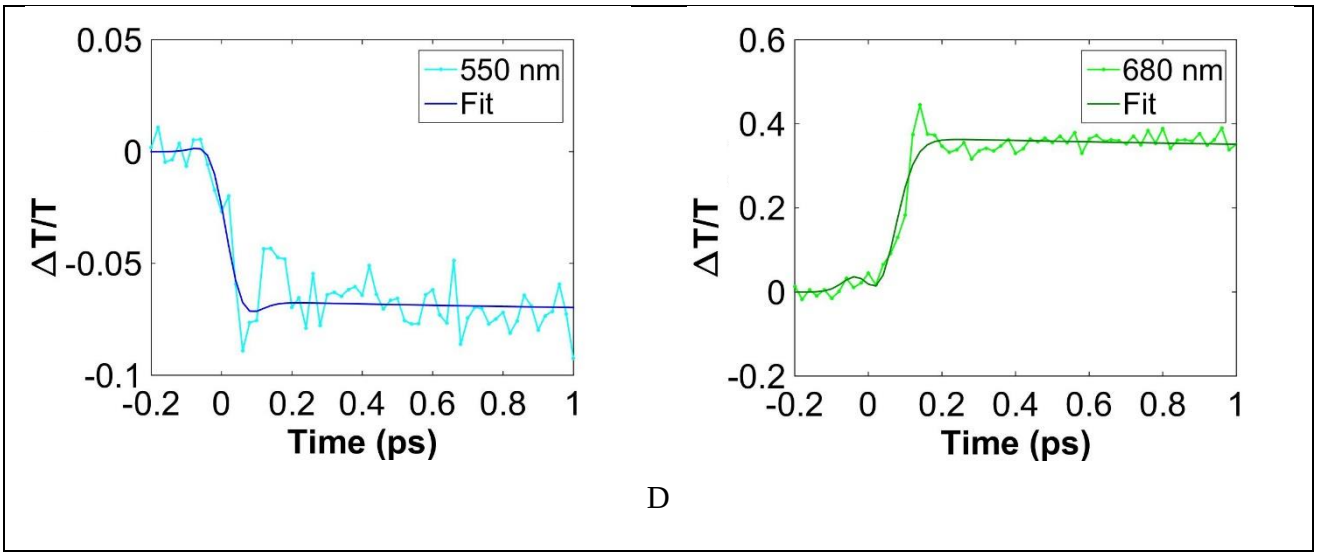

Figure S12. Decay traces and corresponding fittings (in the range 0-300 ps) for the 480, 550 and 680 nm features observed for the dye-sensitized ZrO_2 (A), ATO (B), WO_3 (C) and SnO_2 (D) after the femtosecond laser excitation at 485 nm. The corresponding fittings in the < 1000 fs range are also reported.

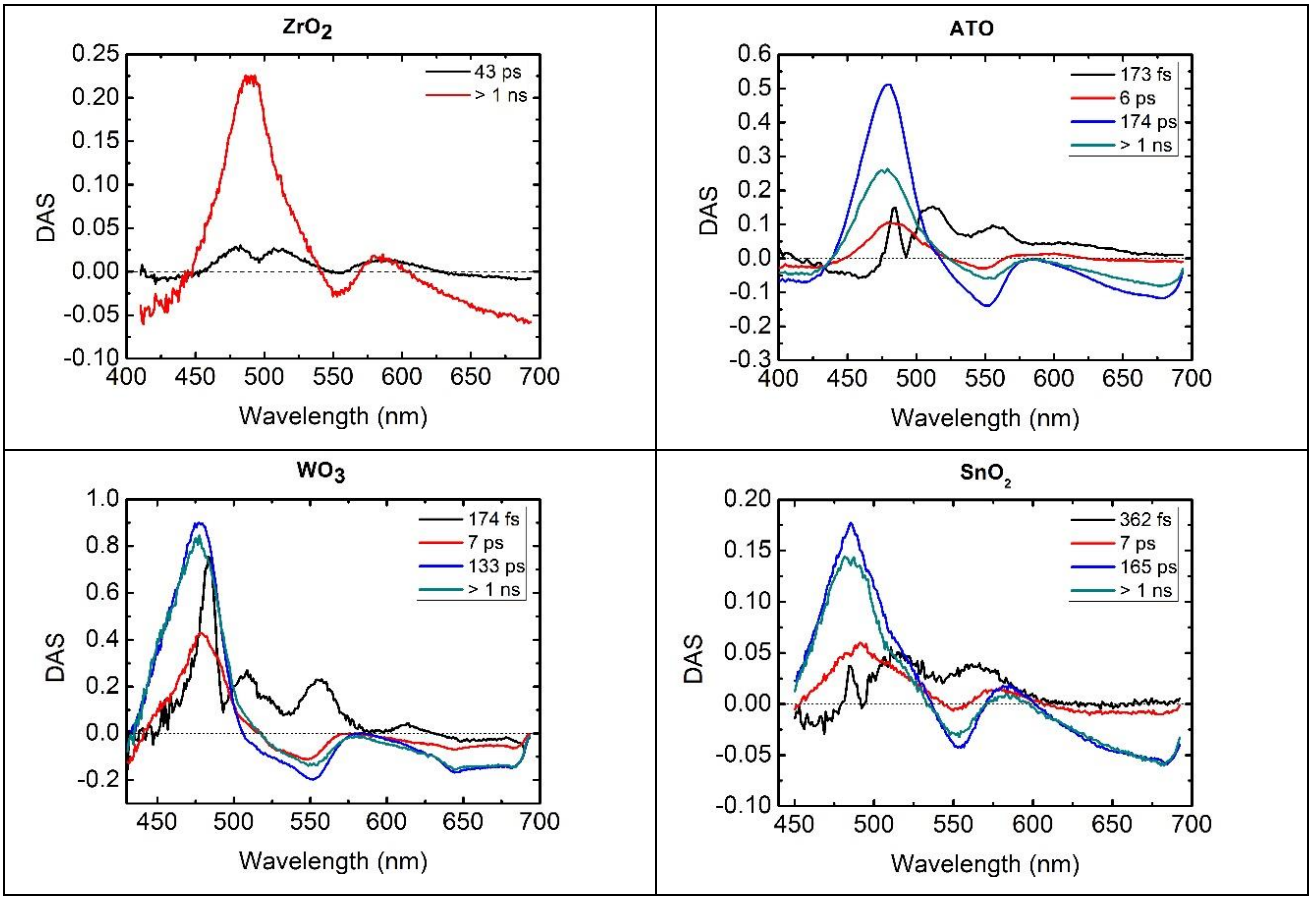

Figure S13. Global analysis of the ΔT/T maps for the dye-sensitized ZrO_2, ATO, WO_3 and SnO_2. For each sample the black and red curves are the decay-associated spectra (DAS), with corresponding time constants indicated in the legend.[4,5]

Table S1. Time constants associated to the formation and recombination of the charge separated species SC(e^-)-PDI(+) after the femtosecond laser excitation of the PDI-sensitized photoanodes.

#	**550 nm initial rise,** ***i.e.*** **SC(e^-)-PDI(+) formation**	**550 nm decay,** ***i.e.*** **SC(e^-)-PDI(+) recombination**
ATO-PDI	τ = 173 ± 8 fs	τ = 174 ± 2 ps
WO_3-PDI	τ = 174 ± 5 fs	τ = 133 ± 1 ps
SnO_2-PDI	τ = 362 ± 12 fs	τ = 165 ± 3 ps

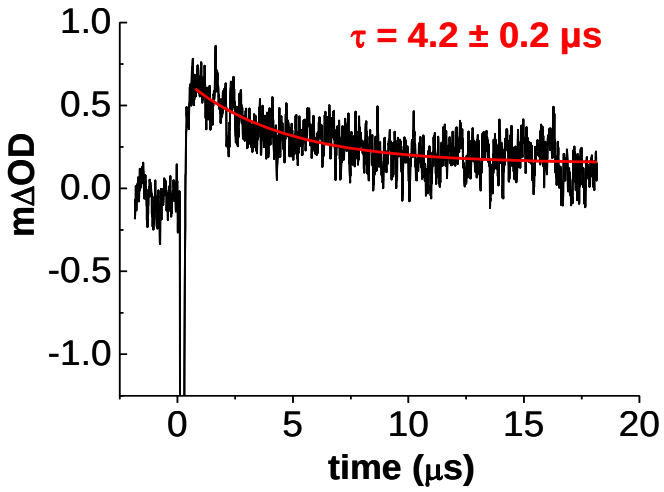

Figure S14. Kinetic evolution of the absorption feature at 550 nm (due to the ATO(e^-)-PDI(+) charge separated state) after the nanosecond laser excitation at 532 nm; 1.48 kV laser pump; average of 60 laser shots, corrected for the pulser baseline; 5 s delay; 350 Ω impedance (300 ns pulse time base). In 0.1 M $NaClO_4$ pH 3.

3.9. Functionalization with IrO_2 WOC

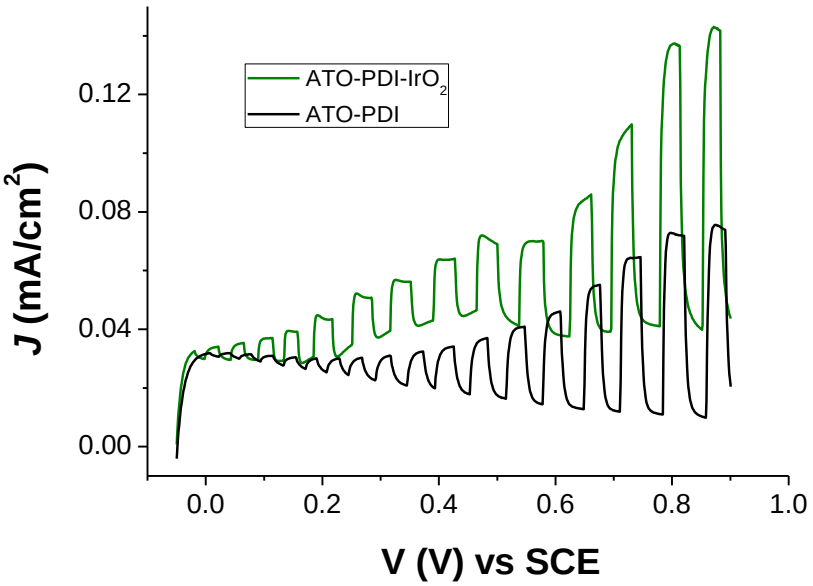

Figure S15. J-V curves of the ATO-PDI photoanodes before (black) and after (green) the functionalization with IrO_2 water oxidation catalyst. In 0.1 M $NaClO_4$ (pH 3); 10 mV/s scan rate; under chopped (B) illumination (0.1 W/cm^2 irradiation power, AM1.5G filter).

---

4. References

[1] Rigodanza, F.; Tenori, E.; Bonasera, A.; Syrgiannis, Z.; Prato, M. Fast and Efficient Microwave-Assisted Synthesis of Perylenebisimides. *Eur. J. Org. Chem.* **2015**, 5060-5063.

[2] Xu, Z.; Cheng, W.; Guo, K.; Yu, J.; Shen, J.; Tang, J.; Yang, W.; Yin, M. Molecular Size, Shape, and Electric Charges: Essential for Perylene Bisimide-Based DNA Intercalator to Localize in Cell Nuclei and Inhibit Cancer Cell Growth. *ACS Appl. Mater. Interfaces* **2015**, *7*, 9784-9791.

[3] Tuntiwechapikul, W.; Taka, T.; Béthencourt, M.; Makonkawkeyoon, L.; Lee, T. R. Interactions of a Platinum-Modified Perylene Derivative with the Human Telomeric G-Quadruplex. *Bioorg. Med. Chem. Lett.* **2006**, *16*, 4120-4126.

[4] van Stokkum, I. H. M.; Larsen, D. S.; van Grondelle, R. Global and Target Analysis of Time-Resolved Spectra. *Biochim. Biophys. Acta* **2004**, *1657*, 82-104.

[5] Snellenburg, J. J.; Laptenok, S. P.; Seger, R.; Mullen, K. M.; van Stokkum, I. H. M. Glotaran: A Java-Based Graphical User Interface for the R Package TIMP. *J. Stat. Software* **2012**, 49, 1-22.